

Cutting Edge: Transcriptional Profiling Reveals Multifunctional and Cytotoxic Antiviral Responses of Zika Virus-Specific CD8⁺ T Cells

Alba Grifoni,^{*} Priscilla Costa-Ramos,[†] John Pham,^{*} Yuan Tian,^{*} Sandy L. Rosales,^{*} Grégory Seumois,^{*} John Sidney,^{*} Aruna D. de Silva,^{*,‡,1} Lakshmanane Premkumar,[§] Matthew H. Collins,^{§,¶} Mars Stone,^{||} Phillip J. Norris,^{||} Claudia M. E. Romero,[#] Anna Durbin,^{**} Michael J. Ricciardi,^{††} Julie E. Ledgerwood,^{‡‡} Aravinda M. de Silva,[§] Michael Busch,^{||} Bjoern Peters,^{*,§§} Pandurangan Vijayanand,^{*} Eva Harris,^{¶¶} Andrew K. Falconar,[#] Esper Kallas,[†] Daniela Weiskopf,^{*} and Alessandro Sette^{*,§§}

Zika virus (ZIKV) constitutes an increasing public health problem. Previous studies have shown that CD8⁺ T cells play an important role in ZIKV-specific protective immunity. We have previously defined antigenic targets of the ZIKV-specific CD8⁺ T cell response in humans. In this study, we characterized the quality and phenotypes of these responses by a combined use of flow cytometry and transcriptomic methods, using PBMCs from donors deriving from different geographical locations collected in the convalescent phase of infection. We show that ZIKV-specific CD8⁺ T cells are characterized by a polyfunctional IFN- γ signature with upregulation of TNF- α , TNF receptors, and related activation markers, such as CD69, as well as a cytotoxic signature characterized by strong upregulation of GZMB and CRTAM. The signature is stable and not influenced by previous dengue virus exposure, geographical location, or time of sample collection postinfection. To our knowledge, this work elucidates the first in-depth characterization of human CD8⁺ T cells responding to ZIKV infection. *The Journal of Immunology*, 2018, 201: 3487–3491.

The relatively recent spread of Zika virus (ZIKV) in the absence of any available treatment or preventative vaccine has illustrated the need to better understand a number of issues associated with this previously understudied virus ranging from epidemiology, disease pathogenesis, and host immune responses. CD8⁺ T cell immune responses seem to play an important role in ZIKV-specific protective immunity, contributing to protective immunity against ZIKV. Dengue virus (DENV)-pre-exposed CD8⁺ T cells are also able to mount cross-protective responses against ZIKV challenge (1, 2). In this context, it is important to study and define the features of ZIKV-specific CD8⁺ T cell responses and ascertain whether these responses are fully functional or somehow altered (especially in DENV-pre-exposed donors), raising the possibility that these responses may be associated with immunopathology. We previously showed that subjects characterized by prior DENV infection displayed not only increased magnitude of ZIKV responses in the acute phase but also showed a skewed immunodominance pattern of responses toward nonstructural proteins as previously observed in the context of DENV infection (3, 4). However, an in-depth

^{*}Division of Vaccine Discovery, La Jolla Institute for Allergy and Immunology, La Jolla, CA 92037; [†]Division of Clinical Immunology and Allergy, School of Medicine, University of São Paulo, São Paulo 01246-903, Brazil; [‡]Genetech Research Institute, Colombo 08, Sri Lanka; [§]Department of Microbiology and Immunology, University of North Carolina School of Medicine, Chapel Hill, NC 27516; [¶]The Hope Clinic, Emory Vaccine Center, Division of Infectious Diseases, Department of Medicine, School of Medicine, Emory University, Decatur, GA 30317; ^{||}Blood Systems Research Institute, San Francisco, CA 94118; ^{||}Universidad del Norte, Barranquilla 1569, Colombia; ^{**}School of Medicine, University of Vermont, Burlington, VT 05405; ^{††}Department of Pathology, Miller School of Medicine, University of Miami, Miami, FL 33146; ^{‡‡}Vaccine Research Center, National Institute of Allergy and Infectious Diseases, Bethesda, MD 20892; ^{§§}University of California San Diego, La Jolla, CA 92093; and ^{¶¶}Division of Infectious Diseases and Vaccinology, School of Public Health, University of California, Berkeley, CA 94720

¹Current address: Department of Paraclinical Sciences, Kotelawala Defense University, Ratmalana, Sri Lanka.

ORCID: 0000-0002-2209-5966 (A.G.); 0000-0002-8164-6852 (G.S.); 0000-0002-0987-405X (J.S.); 0000-0001-5291-9543 (A.D.d.S.); 0000-0001-7974-1933 (M.H.C.); 0000-0001-5619-2767 (M.S.); 0000-0003-0526-2088 (P.J.N.); 0000-0001-7860-5542 (C.M.E.R.); 0000-0002-6652-2851 (A.D.); 0000-0002-1446-125X (M.B.); 0000-0002-8457-6693 (B.P.); 0000-0002-7238-4037 (E.H.); 0000-0002-2066-9487 (A.K.F.); 0000-0003-2026-6925 (E.K.); 0000-0001-7013-2250 (A.S.).

Received for publication August 8, 2018. Accepted for publication October 12, 2018.

This work was supported by National Institutes of Health (NIH) Contracts HHSN272200900042C and HHSN27220140045C, and Grants U19 AI118626-01 to A.S., HHSN2682011000011 to M.B., and S10OD016262 to P.V. Further support was provided by the Zika Preparedness Latin American Network, which has received funding from the European Union's Horizon 2020 research and innovation program under Grant Agreement 734584. Blood donor samples from Puerto Rico and Florida were collected as part of the National Heart, Lung, and Blood Institute Recipient Epidemiology and Donor Evaluation Study-III. The La Jolla Institute for Allergy and Immunology's FACSria II cell sorter was acquired through Shared Instrumentation Grant Program S10 RR027366. The Illumina HiSeq 2500 Sequencer was purchased through NIH S10OD016262.

Address correspondence and reprint requests to Dr. Alessandro Sette, La Jolla, 9420 Athena Circle, La Jolla, CA 92037. E-mail address: alex@lji.org

The online version of this article contains supplemental material.

Abbreviations used in this article: CRTAM, cytotoxic and regulatory T cell molecule; DENV, dengue virus; GZMB, granzyme B; PCA, principal component analysis; TPM, transcript per million; ZIKV, Zika virus.

characterization of the functionality of ZIKV-specific CD8⁺ T cell responses is not available to date.

Materials and Methods

Human blood samples and ZIKV and DENV determination

Blood donations from convalescent donors previously infected with ZIKV were collected (4) in Puerto Rico within the Recipient Epidemiology and Donor Evaluation Study-III or at the University of North Carolina (UNC Institutional Review Board no. 08-0895) and University of Miami from United States travelers with Zika symptoms. An additional cohort was identified at the Universidad del Norte in Barranquilla, Colombia. ZIKV infection was confirmed using RT-PCR during the early acute/symptomatic phase (5). Clinical and serological characteristics are summarized in Supplemental Table I. In addition to positive RT-PCR, previous ZIKV infections in convalescent phase samples were also confirmed using ZIKV neutralization assays, depleting DENV cross-reactive Abs (6). PBMCs were isolated (3), cryopreserved, and stored in liquid nitrogen until usage. DENV seropositivity was determined by DENV IgG or an inhibition ELISA (7, 8).

IFN- γ capture assay, sorting, and flow cytometry

Cells were stimulated with ZIKV peptide pools (4). Additionally, we used 309 ZIKV 9-mers and 10-mers corresponding to previously identified epitopes supplemented with predicted epitopes based on a 27-allele method (9) using TepiTool, available in the Immune Epitope Database and Analysis Resource (www.IEDB.org) (10). IFN- γ -producing cells were captured using a cytokine secretion assay (Miltenyi Biotech, Bergisch Gladbach, Germany) (11). Sorting gating strategy is shown in Supplemental Fig. 1. For the intracellular cytokine staining, PBMCs were cultured 6 h with 1 μ g/ml peptide pools and BD GolgiPlug (BD Biosciences, San Diego, CA), then permeabilized, stained, and analyzed using FlowJo software (4). Supplemental Table II shows the Abs used for sorting and flow cytometry experiments.

RNA sequencing, bioinformatics, and statistical data analysis

Two hundred cells for each condition were collected. To generate full-length transcriptomes from the low cells per sample, we adapted the Smart-Seq2 protocol (12). Bioinformatics analysis to obtain the raw counts and differentially expressed genes were performed as previously described (13). We considered genes to be differentially expressed with an adjusted p value of <0.05 and the log₂ fold change in gene expression >1 . Only genes with an average transcript per million (TPM) count ≥ 10 in ZIKV IFN- γ ⁺ condition have been considered for further analysis. Principal component analysis (PCA) was performed on the top 500 most variable genes using *vsust* transformation and the “*prcomp*” function in R, setting “*scale*” equal to TRUE. The heatmap was generated on *vsust*-transforming data using *Qlucore*. Statistical analyses for FACS experiments were performed using Prism 7 (GraphPad Software, San Diego, CA). One-tailed Mann-Whitney or Wilcoxon tests were applied when appropriate. The data have been deposited in the Gene Expression Omnibus (GSE105884, <http://www.ncbi.nlm.nih.gov/geo/>) and ImmPort (SDY903, <http://www.immport.org/>).

Results and Discussion

To examine the nature of CD8⁺ T cell responses recognizing ZIKV epitopes, we performed a transcriptomic analysis of PBMCs from ZIKV-infected donors collected at the convalescent phase. In this study, PBMCs were stimulated *ex vivo* with ZIKV-specific peptide pools, and Ag-specific CD8⁺ T cells were sorted based on their ability to produce IFN- γ . The patients' CD8⁺ T cells that did not produce IFN- γ in response to epitope stimulation from these same cultures as well as total unstimulated CD8⁺ T cells were also collected for comparison with their ZIKV-specific IFN- γ -producing CD8⁺ T cells. After sorting, microscaled RNA sequence determinations were performed on low cell numbers (12). We then analyzed the global gene expression patterns using PCA of the 500 most variable genes obtained after RNA sequencing (Fig. 1A). Unstimulated and ZIKV-stimulated IFN- γ ⁻ CD8⁺ T cells clustered together and were clearly separated from the gene expression profiles of the ZIKV-stimulated IFN- γ ⁺ CD8⁺ T cells. This suggested that the main component of human CD8⁺ T cell

response to ZIKV epitopes were from their IFN- γ -producing cells, in agreement with previous studies on both ZIKV and the closely related DENV regarding CD8 responses (1, 3, 4, 14, 15). The IFN- γ ⁻ CD8⁺ T cells may also include some, if not many, ZIKV-specific T cells, which did not secrete IFN- γ but instead secreted IL-2 or TNF- α under the stimulation of peptides. Further experiments targeting cell subpopulations secreting other cytokines or selected on the basis of specific activation markers could be performed in the future to broaden the characterization of ZIKV-specific CD8⁺ T cell responses.

The interplay between ZIKV and DENV is an important issue because ZIKV and DENV not only share a high level of protein sequence homology but are also transmitted by the same mosquitoes, and ZIKV transmission has predominantly occurred in DENV-endemic areas (16). We have previously shown that prior DENV exposure modulates ZIKV responses when comparing acute samples that were DENV naive or previously exposed (4). In this study, we do not observe differences both in terms of frequency of IFN- γ ⁺ cells of DENV seronegative and seropositive (Supplemental Fig. 1B) as well as in terms of gene expression observed (Fig. 1A), suggesting that DENV pre-exposure might affect ZIKV CD8⁺ T cells only during the acute phase of the infection. These preliminary findings should be further explored; however, they are in agreement with previous work in which small differences in monocyte gene expression profiles were observed in patients who had ZIKV or DENV infections, suggesting similarities between the two viral infections at the gene expression level (17).

To identify gene expression patterns associated with ZIKV-specific CD8⁺ T cell responses, we determined the differential gene expression profiles of the patients' IFN- γ ⁻ and IFN- γ ⁺ cells after ZIKV peptide pools stimulation and on IFN- γ ⁻ cells that were unstimulated or stimulated with ZIKV (Fig. 1B). Overall, a total of 153 genes were differentially expressed in either one of these two analyses. Of these, 142 genes were upregulated at least 2-fold in the IFN- γ ⁺ compared with the IFN- γ ⁻ ZIKV-stimulated cells, and 32 genes were differentially upregulated at a more stringent cutoff of a 4-fold level in IFN- γ ⁺ compared with IFN- γ ⁻ cells (Fig. 1C). These results further emphasize that the main component of CD8⁺ responses to ZIKV peptides were the IFN- γ -producing cells (4).

Next, we more closely inspected the mRNA sequence profiles of the IFN- γ ⁺ CD8⁺ T cells to ascertain which genes at a more stringent 4-fold change cutoff were upregulated in the ZIKV-specific CD8⁺ T cells (Fig. 1C). Interestingly, among the most significantly upregulated genes were those encoding granzyme B (*GZMB*) and cytotoxic and regulatory T cell molecule (*CRTAM*), implying that the CD8 responses were not limited to cytokine release but were also associated with the hallmarks of a cytotoxic response (18). Among the other strongly upregulated genes were those associated with cellular activation, such as tumor necrosis receptor superfamily member 9 (*TNFRSF9*), which encodes the CD137 protein (also known as 4-1BB), important in priming and promoting CD8⁺ T cell effector and memory functions in the context of viral infection (19), and *CD69*, which encodes an important marker of T cell activation. In addition, significant upregulation was also noted for *NFKBID*, which encodes an NF known to be involved in homeostasis of the immune

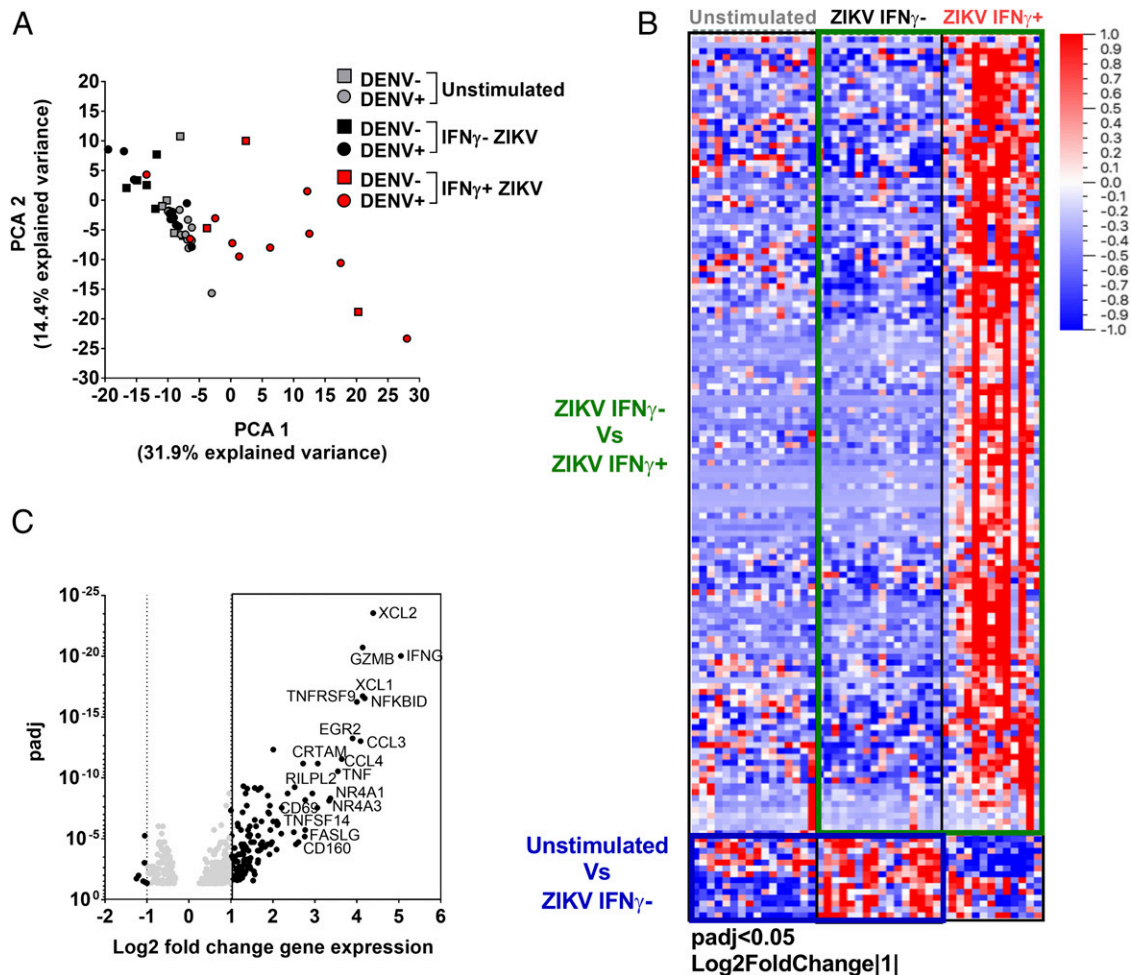


FIGURE 1. Gene expression analysis of ZIKV-specific CD8⁺ T cells. **(A)** PCA of unstimulated IFN- γ ⁻ (gray) and ZIKV-stimulated IFN- γ ⁻ (black) and IFN- γ ⁺ (red). DENV pre-exposed (circles) and DENV naive (square) are also shown **(B)**. Heatmap of differentially expressed genes after comparison of IFN- γ ⁻ and IFN- γ ⁺ cells stimulated with ZIKV pools. **(C)** Differentially expressed genes based on adjusted *p* value and log₂ fold change gene expression. Genes with log₂ fold change >2 are highlighted.

system that is activated after TCR stimulation (20). Other upregulated genes that correlated with activation were TNF ligand superfamily member 6/Fas ligand gene (*TNFSF6/FASLG*) and member 14 (*TNFSF14/CD258*), which encode proteins involved in cytotoxic T cell apoptotic processes and immune regulation, and *ERG2*, encoding an upstream regulator of effector CD4⁺ and CD8⁺ T cells linked with protective responses and limiting immunopathology (21) as well as with regulating CD8⁺ T cell activation (22).

Other prominently upregulated genes were X-C motif chemokine ligand 1 and 2 (*XCL1* and *XCL2*), which encode chemokines with inflammatory function that are known to induce leukocyte migration and activation (23). The genes encoding the chemokine (C-C motif) ligand 3 and 4 (*CCL3* and *CCL4*) proteins, associated with inflammation and in the case of *CCL3* also with CD8 effector function, were also upregulated (24).

Based on the gene function described above and available in UniProt knowledgebase database (<https://www.uniprot.org/>), we functionally grouped together the genes more strongly upregulated in ZIKV-specific CD8⁺ T cell genes into five main groups: 1) polyfunctional cytokines, 2) cytotoxicity, 3) T cell activation and regulation, 4) proinflammation, and 5) T cell homing.

We previously reported, using a different cohort of donors/samples, that ZIKV-specific CD8⁺ T cell responses were characterized by IFN- γ , TNF- α , and GZMB release (4). We then compared the geometric mean of fluorescence intensity expression of IFN- γ , TNF- α , and GZMB in IFN- γ ⁻ and IFN- γ ⁺ cell groups, reanalyzing our previously published data (4) (Supplemental Fig. 2B, 2D, 2F), to the TPM count originated by the mRNA sequence determinations performed in the current study. All genes (*IFN- γ* , *TNF- α* , and *GZMB*) encoding the proteins found to be upregulated by FACS analysis in previous studies were also found to be upregulated at the mRNA level in this study (Supplemental Fig. 2C, 2E, 2G). To further validate the CD8⁺ T cell ZIKV signature obtained by the mRNA sequence determinations and analyses, we selected six additional proteins (CD137, CD258, FASLG, CCL3, CRTAM, and CD69) based on differential expression of their corresponding genes (changes of >4-fold, *p*-adjusted values <0.05) (Fig. 1C) and the availability of a suitable commercial mAb to detect them. The protein-level expression of these markers was determined on a set of 12 donors known to respond to stimulation with ZIKV peptides, as previously reported (4), after a 6-h stimulation period with ZIKV-specific pooled peptides and intracellular staining. Overall, there was a good correlation between

upregulation at the mRNA (Fig. 2A) and protein (Fig. 2B) expression levels. Our results demonstrated that the CD8⁺ T cell responses recognizing ZIKV-specific epitopes were prevalently associated with IFN- γ ⁺ cells, as expected from our experimental strategy, and that this response appeared to be fully functional, as demonstrated by the upregulation of genes involved in cytotoxicity, chemotaxis, and inflammation. To prove that these observations were generally applicable regardless of the particular cohort analyzed or the time elapsed postinfection, we also analyzed the same markers on PBMCs from a different cohort in Barranquilla (Colombia) that had been collected 1–2 y after ZIKV infection. This independent ZIKV cohort showed patterns of protein upregulation remarkably similar to those detected in the previous cohort (Fig. 2C). These data, therefore, demonstrated that this expression signature was both reproducible and temporally stable after Ag-specific stimulation even 1–2 y after ZIKV infection. In summary, we report, to our knowledge, the first human immune profile of CD8⁺ T cells after ZIKV Ag-specific stimulation. Our data show that ZIKV-specific CD8⁺ T cell responses were predominantly associated with

IFN- γ responses and that their gene expression signatures were further associated with cytokine polyfunctionality and cytotoxic activity. These common features were independent of DENV pre-exposure, geographical location, or time of sample collection postinfection and were identified both at the mRNA and protein level, therefore making these suitable candidates to be evaluated in cellular vaccine-induced immune responses. Because of the small volume of samples available, we focused our study on immune profiling of ZIKV-specific CD8⁺ T cells. Future studies will address the immune profiles of human ZIKV-specific CD4⁺ T cells and compare the functionalities of CD4⁺ T cells with the ones of CD8⁺ T cells. Indeed, recent studies in humans and mouse models have shown the importance of ZIKV-specific CD4⁺ T cells in protecting from severe ZIKV severe and Ab development (25–27). Additionally, it would be of interest to test whether disease severity during the acute phase impacts the gene transcription and protein expression in ZIKV-specific T cells. However, the cohorts studied in this study were mostly characterized by a mild form of ZIKV disease and, therefore, this analysis could not be performed based on

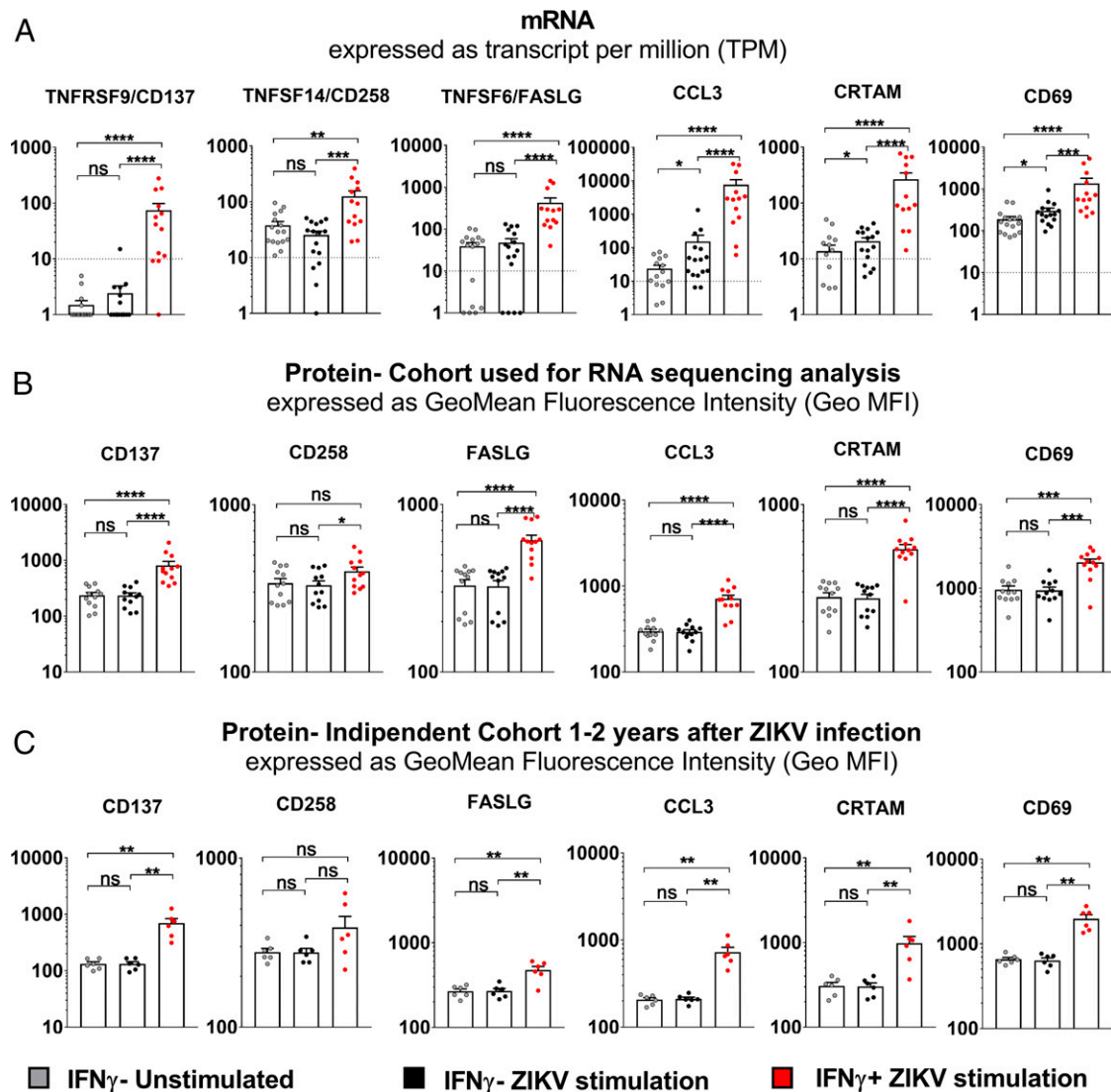


FIGURE 2. Correlation of expression at the mRNA and protein levels in CD8⁺ T cells of selected markers. **(A)** TPM for *CD137*, *CD258*, *FASLG*, *CCL3*, *CRTAM*, and *CD69* genes. **(B and C)** Geometric mean of fluorescence intensity for intracellular protein level determinations (B). ZIKV-independent cohort collected 1–2 y postinfection (C). * $p < 0.05$, ** $p < 0.01$, *** $p < 0.001$, **** $p < 0.0001$.

the current cohort. In conclusion, the current study represents a baseline for comparison between different clinical outcomes of ZIKV infection in the CD8⁺ T cell context.

Acknowledgments

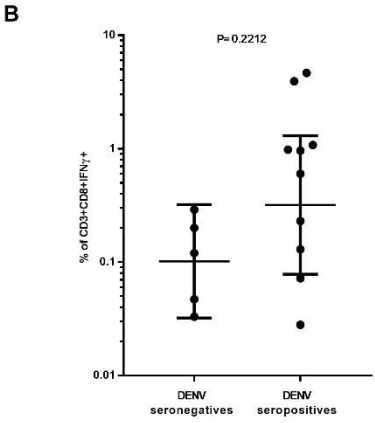
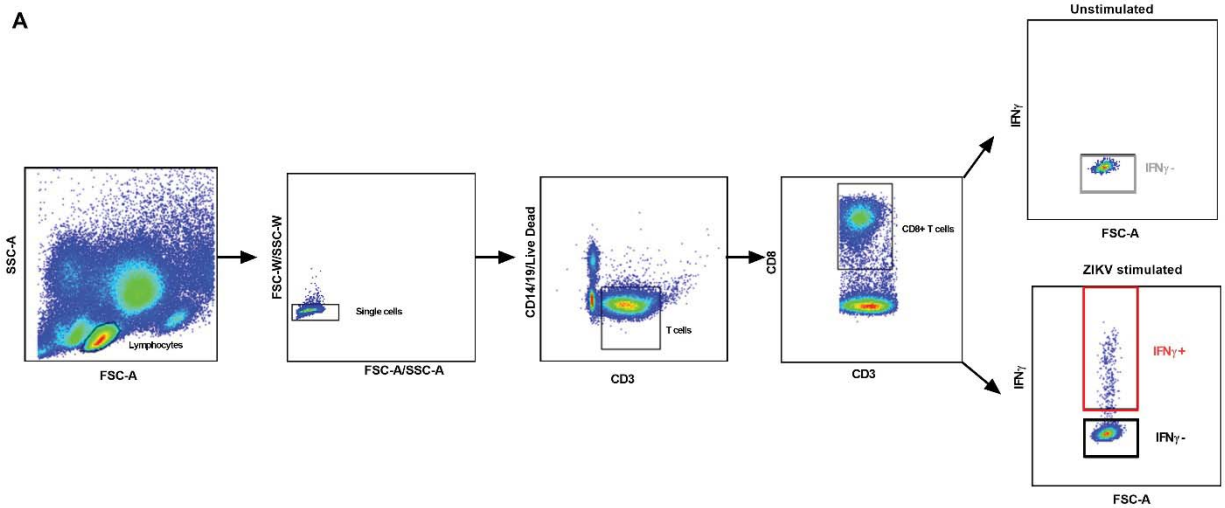
We thank Sheridan Martini for sample coordination, Ashmita Loganda and Jason Greenbaum of the Bionformatic Core, and Denise Hinz and Cheryl Kim of the Flow Cytometry Core at the La Jolla Institute for Allergy and Immunology.

Disclosures

The authors have no financial conflicts of interest.

References

1. Elong Ngono, A., E. A. Vizcarra, W. W. Tang, N. Sheets, Y. Joo, K. Kim, M. J. Gorman, M. S. Diamond, and S. Shresta. 2017. Mapping and role of the CD8⁺ T cell response during primary Zika virus infection in mice. *Cell Host Microbe* 21: 35–46.
2. Wen, J., A. Elong Ngono, J. A. Regla-Nava, K. Kim, M. J. Gorman, M. S. Diamond, and S. Shresta. 2017. Dengue virus-reactive CD8⁺ T cells mediate cross-protection against subsequent Zika virus challenge. *Nat. Commun.* 8: 1459.
3. Weiskopf, D., M. A. Angelo, E. L. de Azeredo, J. Sidney, J. A. Greenbaum, A. N. Fernando, A. Broadwater, R. V. Kolla, A. D. De Silva, A. M. de Silva, et al. 2013. Comprehensive analysis of dengue virus-specific responses supports an HLA-linked protective role for CD8+ T cells. *Proc. Natl. Acad. Sci. USA* 110: E2046–E2053.
4. Grifoni, A., J. Pham, J. Sidney, P. H. O'Rourke, S. Paul, B. Peters, S. R. Martini, A. D. de Silva, M. J. Ricciardi, D. M. Magnani, et al. 2017. Prior dengue virus exposure shapes T cell immunity to Zika virus in humans. *J. Virol.* DOI: 10.1128/JVI.01469-17.
5. Waggoner, J. J., L. Gresh, A. Mohamed-Hadley, G. Ballesteros, M. J. Davila, Y. Tellez, M. K. Sahoo, A. Balmaseda, E. Harris, and B. A. Pinsky. 2016. Single-reaction multiplex reverse transcription PCR for detection of Zika, chikungunya, and dengue viruses. *Emerg. Infect. Dis.* 22: 1295–1297.
6. Collins, M. H., E. McGowan, R. J. J. Young, C. A. Lopez, R. S. Baric, H. M. Lazear, and A. M. de Silva. 2017. Lack of durable cross-neutralizing antibodies against Zika virus from dengue virus infection. *Emerg. Infect. Dis.* 23: 773–781.
7. Kanakarathne, N., W. M. Wahala, W. B. Messer, H. A. Tissera, A. Shahani, N. Abeyasinghe, A. M. de-Silva, and M. Gunasekera. 2009. Severe dengue epidemics in Sri Lanka, 2003–2006. *Emerg. Infect. Dis.* 15: 192–199.
8. Fernández, R. J., and S. Vázquez. 1990. Serological diagnosis of dengue by an ELISA inhibition method (EIM). *Mem. Inst. Oswaldo Cruz* 85: 347–351.
9. Paul, S., D. Weiskopf, M. A. Angelo, J. Sidney, B. Peters, and A. Sette. 2013. HLA class I alleles are associated with peptide-binding repertoires of different size, affinity, and immunogenicity. *J. Immunol.* 191: 5831–5839.
10. Paul, S., J. Sidney, A. Sette, and B. Peters. 2016. TepiTool: a pipeline for computational prediction of T cell epitope candidates. *Curr. Protoc. Immunol.* 114: 18.19.1–18.19.24.
11. Hinz, D., G. Seumois, A. M. Gholami, J. A. Greenbaum, J. Lane, B. White, D. H. Broide, V. Schulten, J. Sidney, P. Bakhrui, et al. 2016. Lack of allergy to timothy grass pollen is not a passive phenomenon but associated with the allergen-specific modulation of immune reactivity. *Clin. Exp. Allergy* 46: 705–719.
12. Rosales, S. L., S. Liang, I. Engel, B. J. Schmiedel, M. Kronenberg, P. Vijayanand, and G. Seumois. 2018. A sensitive and integrated approach to profile messenger RNA from samples with low cell numbers. *Methods Mol. Biol.* 1799: 275–301.
13. Tian, Y., M. Babor, J. Lane, V. Schulten, V. S. Patil, G. Seumois, S. L. Rosales, Z. Fu, G. Picarda, J. Burel, et al. 2017. Unique phenotypes and clonal expansions of human CD4 effector memory T cells re-expressing CD45RA. *Nat. Commun.* 8: 1473.
14. Lum, F. M., D. C. B. Lye, J. J. L. Tan, B. Lee, P. Y. Chia, T. K. Chua, S. N. Amrun, Y. W. Kam, W. X. Yee, W. P. Ling, et al. 2018. Longitudinal study of cellular and systemic cytokine signatures to define the dynamics of a balanced immune environment during disease manifestation in Zika virus-infected patients. *J. Infect. Dis.* 218: 814–824.
15. de Alwis, R., D. J. Bangs, M. A. Angelo, C. Cerpas, A. Fernando, J. Sidney, B. Peters, L. Gresh, A. Balmaseda, A. D. de Silva, et al. 2016. Immunodominant dengue virus-specific CD8+ T cell responses are associated with a memory PD-1+ phenotype. *J. Virol.* 90: 4771–4779.
16. World Health Organization. 2017. Situation report: Zika virus microcephaly Guillain-Barré syndrome. Available at: <http://apps.who.int/iris/bitstream/handle/10665/253604/zikasitrep20Jan17-eng.pdf;jsessionid=64AF3C2F78E08372CD2E090CC063A504?sequence=1>. Accessed: January 20, 2017.
17. Michlmayr, D., P. Andrade, K. Gonzalez, A. Balmaseda, and E. Harris. 2017. CD14⁺CD16⁺ monocytes are the main target of Zika virus infection in peripheral blood mononuclear cells in a paediatric study in Nicaragua. *Nat. Microbiol.* 2: 1462–1470.
18. Takeuchi, A., Y. Itoh, A. Takumi, C. Ishihara, N. Arase, T. Yokosuka, H. Koseki, S. Yamasaki, Y. Takai, J. Miyoshi, et al. 2009. CRTAM confers late-stage activation of CD8+ T cells to regulate retention within lymph node. *J. Immunol.* 183: 4220–4228.
19. Yoshimori, M., K. Imadome, H. Komatsu, L. Wang, Y. Saitoh, S. Yamaoka, T. Fukuda, M. Kurata, T. Koyama, N. Shimizu, et al. 2014. CD137 expression is induced by Epstein-Barr virus infection through LMP1 in T or NK cells and mediates survival promoting signals. *PLoS One* 9: e112564.
20. Schuster, M., M. Annemann, C. Plaza-Sirvent, and I. Schmitz. 2013. Atypical IκB proteins - nuclear modulators of NF-κB signaling. *Cell Commun. Signal.* 11: 23.
21. Miao, T., A. L. J. Symonds, R. Singh, J. D. Symonds, A. Ogbe, B. Omodho, B. Zhu, S. Li, and P. Wang. 2017. Egr2 and 3 control adaptive immune responses by temporally uncoupling expansion from T cell differentiation. *J. Exp. Med.* 214: 1787–1808.
22. Mauri, D. N., R. Ebner, R. I. Montgomery, K. D. Kochel, T. C. Cheung, G. L. Yu, S. Ruben, M. Murphy, R. J. Eisenberg, G. H. Cohen, et al. 1998. LIGHT, a new member of the TNF superfamily, and lymphotoxin alpha are ligands for herpesvirus entry mediator. *Immunity* 8: 21–30.
23. Lei, Y., and Y. Takahama. 2012. XCL1 and XCR1 in the immune system. *Microbes Infect.* 14: 262–267.
24. Trifilo, M. J., C. C. Bergmann, W. A. Kuziel, and T. E. Lane. 2003. CC chemokine ligand 3 (CCL3) regulates CD8(+)-T-cell effector function and migration following viral infection. *J. Virol.* 77: 4004–4014.
25. Hassert, M., K. J. Wolf, K. E. Schwery, R. J. DiPaolo, J. D. Brien, and A. K. Pinto. 2018. CD4+ T cells mediate protection against Zika associated severe disease in a mouse model of infection. *PLoS Pathog.* 14: e1007237.
26. Lucas, C. G. O., J. Z. Kitoko, F. M. Ferreira, V. G. Suzart, M. P. Papa, S. V. A. Coelho, C. B. Cavazzoni, H. A. Paula-Neto, P. C. Olsen, A. Iwasaki, et al. 2018. Critical role of CD4⁺ T cells and IFNγ signaling in antibody-mediated resistance to Zika virus infection. *Nat. Commun.* 9: 3136.
27. Koblishcke, M., K. Stiasny, S. W. Aberle, S. Malafa, G. Tschouchnikas, J. Schwaiger, M. Kundi, F. X. Heinz, and J. H. Aberle. 2018. Structural influence on the dominance of virus-specific CD4 T cell epitopes in Zika virus infection. [Published erratum appears in 2018 *Front Immunol.* 9: 2083.] *Front. Immunol.* 9: 1196.

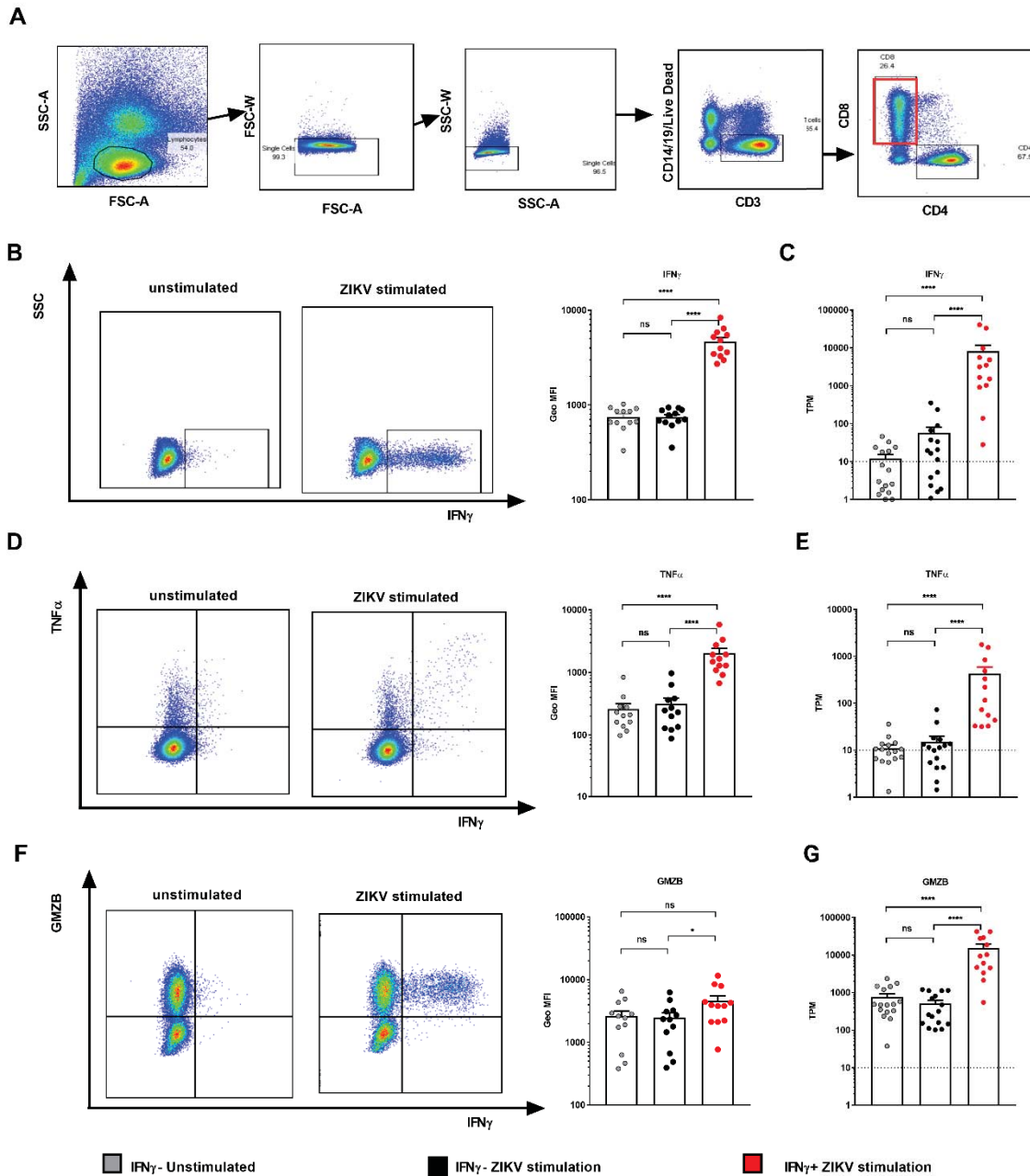


1

2 **Supplemental Fig 1. CD8+ T cell sorting and mRNA sequence determinations and analyses. (A)**

3 Gating strategy. Lymphocytes have been gated based on FSC-A and SSC-A parameters. Single cells have
 4 been derived based first on combination of FSC-A and FSC-W parameters and then SSC-A and SSC-W
 5 parameters. The resulting single cells have been gated for being positive for CD3 and negative for
 6 CD14/19/Live and Dead to obtain the T cells. The resulting T cells have been further gated based on CD8
 7 expression to obtain CD8+ T cells. CD8+ T cells have been further divided based on IFN γ expression.

8 Unstimulated cells have been sorted as IFN γ -CD8+ T cells, while both IFN γ - and IFN γ + CD8+ T cells
 9 stimulated with ZIKV have been collected. (B) Frequency of CD3+CD8+IFN γ + cells after ZIKV stimulation
 10 in DENV seronegative and DENV seropositive donors used for sorting experiments. Statistical analyses
 11 have been performed with Mann-Whitney test.



1

2 **Supplemental Fig 2. Correlations between protein and mRNA expression levels from CD8+ T cells.**

3 (A) Gating strategy. (B, D, F) Representative dot plots and Geo MFI calculated for the IFN γ , TNF α and
 4 granzyme B markers based on previously published data⁸. (C, E, G) transcripts per million (TPM) for the
 5 expression levels of the *IFN γ* , *TNF α* and *granzyme B* encoding genes.

Donor ID	Country of origin	Type of experiment	Days after clinical diagnosis	ZIKV status	DENV status ^{a)}	Clinical Observation
2692	US travellers	RNA sequencing	365	convalescent	pos	not severe
3039	Puerto Rico	RNA sequencing	90	convalescent	pos	not severe
3043	Puerto Rico	RNA sequencing	90	convalescent	pos	not severe
3047	Puerto Rico	RNA sequencing	90	convalescent	pos	not severe
3052	Puerto Rico	RNA sequencing	90	convalescent	pos	not severe
3028	US travellers	RNA sequencing	24	convalescent	pos	not determined
3031	US travellers	RNA sequencing	45	convalescent	pos	not determined
2653	US travellers	RNA sequencing	365	convalescent	neg	not severe
3030	US travellers	RNA sequencing	60	convalescent	neg	not determined
3053	Puerto Rico	RNA sequencing	90	convalescent	neg	not severe
3054	Puerto Rico	RNA sequencing	90	convalescent	neg	not severe
3027	US travellers	RNA sequencing /validation	150	convalescent	pos	not determined
3038	Puerto Rico	RNA sequencing /validation	90	convalescent	pos	not severe
3037	Puerto Rico	RNA sequencing /validation	90	convalescent	pos	not severe
3045	Puerto Rico	RNA sequencing /validation	90	convalescent	pos	not severe
2894	US travellers	RNA sequencing /validation	90	convalescent	neg	not severe
3126	Puerto Rico	validation	90	convalescent	pos	not severe
3127	Puerto Rico	validation	90	convalescent	pos	not severe
3128	Puerto Rico	validation	90	convalescent	pos	not severe
3129	Puerto Rico	validation	90	convalescent	pos	not severe
3130	Puerto Rico	validation	90	convalescent	pos	not severe
3131	Puerto Rico	validation	90	convalescent	pos	not severe
3132	Puerto Rico	validation	90	convalescent	pos	not severe
3421	Colombia	validation	475	convalescent	pos	Guillain-Barré Syndrome
3422	Colombia	validation	565	convalescent	pos	Guillain-Barré Syndrome
3423	Colombia	validation	565	convalescent	pos	not severe
3424	Colombia	validation	505	convalescent	pos	not severe
3428	Colombia	validation	535	convalescent	pos	Guillain-Barré Syndrome
3430	Colombia	validation	595	convalescent	pos	not severe

1 ^{a)} Previous exposure to DENV (Positive or Negative) was determined by the presence of detectable DENV-specific IgG titers.

2

3 **Supplementary Table S1.** List of ZIKV positive donors in convalescent phase, confirmed either by RT-

4 PCR and/or ZIKV serology after serum depletion.

Target	Color	Vendor	Clone	species	reactivity	Experiment
CD14	V500	BD Biosciences	M5E2	mouse	human	Sorting/Flow cytometry
CD19	V500	BD Biosciences	HIB19	mouse	human	Sorting/Flow cytometry
Live/Dead	ef506	eBioscience				Sorting/Flow cytometry
CD3	AF700	eBioscience	UCHT1	mouse	human	Sorting/Flow cytometry
CCR7	PerCP Cy5.5	Biolegend	G043H7	mouse	human	Sorting
CD45RA	ef450	eBioscience	HI100	mouse	human	Sorting
CD8	BV650	BioLegend	RPA-T8	mouse	human	Sorting/Flow cytometry
CD4	APCef780	eBioscience	RPA-T4	mouse	human	Sorting/Flow cytometry
IFN γ	APC-CY7	BioLegend	4S.B3	Mouse	human	Flow cytometry
CD69	PE Cy7	eBioscience	FN50	Mouse	human	Flow cytometry
CD137 (4-1BB)	APC	BioLegend	4B4-1	Mouse	human	Flow cytometry
CD355 (CRTAM)	PE/Cy7	ebioscience	Cr24.1	Mouse	human	Flow cytometry
CD178 (Fas-L)	PE	Biolegend	NOK-1	Mouse	human	Flow cytometry
CD258 (LIGHT)	AF647	BD Biosciences	115520	Mouse	human	Flow cytometry
CCL3	PE	ebioscience	CR3M	Mouse	human	Flow cytometry

1

2 **Supplementary Table S2.** List of monoclonal antibody used for Sorting and Flow cytometry validation

3 experiments.